

# Polyamorphism in vapor-deposited 2-methyltetrahydrofuran: A broadband dielectric relaxation study

Cite as: J. Chem. Phys. 154, 024502 (2021); doi: 10.1063/5.0035591

Submitted: 29 October 2020 • Accepted: 17 December 2020 •

Published Online: 8 January 2021



View Online



Export Citation



CrossMark

Jan Philipp Gabriel,<sup>1,a)</sup> Birte Riechers,<sup>2</sup> Erik Thoms,<sup>1</sup> Anthony Guiseppi-Elie,<sup>3</sup> Mark D. Ediger,<sup>4</sup> and Ranko Richert<sup>1,b)</sup>

## AFFILIATIONS

<sup>1</sup>School of Molecular Sciences, Arizona State University, Tempe, Arizona 85287, USA

<sup>2</sup>Glass and Time, IMFUFA, Department of Science and Environment, Roskilde University, DK-4000 Roskilde, Denmark

<sup>3</sup>Department of Biomedical Engineering, Texas A&M University, College Station, Texas 77843, USA

<sup>4</sup>Department of Chemistry, University of Wisconsin-Madison, Madison, Wisconsin 53706, USA

<sup>a)</sup> Author to whom correspondence should be addressed: JPGabriel@asu.edu

<sup>b)</sup> Electronic mail: Ranko.Richert@asu.edu

## ABSTRACT

Depositing a simple organic molecular glass-former 2-methyltetrahydrofuran (MTHF) onto an interdigitated electrode device via physical vapor deposition gives rise to an unexpected variety of states, as revealed by dielectric spectroscopy. Different preparation parameters, such as deposition temperature, deposition rate, and annealing conditions, lead, on the one hand, to an ultrastable glass and, on the other hand, to a continuum of newfound further states. Deposition below the glass transition temperature of MTHF leads to loss profiles with shape parameters and peak frequencies that differ from those of the known bulk MTHF. These loss spectra also reveal an additional process with Arrhenius-like temperature dependence, which can be more than four decades slower than the main structural relaxation peak. At a given temperature, the time constants of MTHF deposited between 120 K and 127 K span a range of more than three decades and their temperature dependencies change from strong to fragile behavior. This polyamorphism involves at least three distinct states, each persisting for a duration many orders of magnitude above the dielectric relaxation time. These results represent a significant expansion of a previous dielectric study on vapor deposited MTHF [B. Riechers *et al.*, J. Chem. Phys. **150**, 214502 (2019)]. Plastic crystal states and the effects of weak hydrogen bonding are discussed as structural features that could explain these unusual states.

Published under license by AIP Publishing. <https://doi.org/10.1063/5.0035591>

## I. INTRODUCTION

Many molecular liquids are capable of entering the supercooled state by avoiding crystallization even at moderate cooling rates. A characteristic of these liquids is the strong temperature dependence of transport coefficients, which can change more than ten orders of magnitude between the glass transition temperature,  $T_g$ , and the melting temperature,  $T_m$ . For simple liquids (excluding monohydric alcohols), there is no significant change in structure between  $T_g$  and  $T_m$ , but a gradual change in

density. For practically all systems, preparing a supercooled liquid at a given temperature and pressure will always result in the same quasi-equilibrium structure and dynamics. Few examples are known where this rule is violated by polyamorphism, which refers to the existence of multiple long-lived metastable liquid states of the same chemical compound.<sup>1</sup> Well studied cases of polyamorphism are those of triphenyl phosphite,<sup>2</sup> *d*-mannitol,<sup>3–5</sup> and *n*-butanol.<sup>6</sup> Among the plastic crystal forming materials, ethanol and succinonitrile/glutaronitrile mixtures are special cases of displaying both the disordered supercooled liquid and the plastic crystal state.<sup>7,8</sup> While

these materials can assume two distinct structural states with orientational degrees of freedom, their cases would not be considered polyamorphism.

Preparing glasses and liquids by physical vapor deposition (PVD) has expanded the list of materials that show more than one metastable liquid state. Examples are glycerol and similar polyols,<sup>9,10</sup> 4-methyl-3-heptanol,<sup>11</sup> and 2-methyltetrahydrofuran (MTHF).<sup>12</sup> Vapor deposition of organic molecular materials onto substrates held at a temperature around  $0.85T_g$  is known to generate glasses with exceptional properties, such as high kinetic stability, high density, low entropy, low enthalpy, and anisotropy.<sup>13</sup> However, the roles of these properties in promoting polyamorphism in materials obtained by PVD are unclear. Obviously, the formation of a glass via PVD is very different from cooling the bulk liquid, as PVD can combine a low temperature,  $T < T_g$ , with a mobility at the surface that is orders of magnitude higher than that in the bulk at the same temperature. As a result, preparing a glass by vapor deposition can lead to a very different outcome relative to cooling the bulk liquid below its  $T_g$ .

Relative to what is obtained by cooling the melt, the less stable states of PVD-induced polyamorphism are characterized by different features. In the case of glycerol, a fourfold higher dielectric relaxation amplitude and somewhat slower dynamics have been observed.<sup>9,10</sup> A tenfold higher dielectric relaxation amplitude has been found for the monohydric alcohol 4-methyl-3-heptanol, consistent with a Kirkwood correlation factor<sup>14</sup> near  $g_K = 1$ , whereas the ring-like superstructure of hydrogen-bonded molecules gives rise to  $g_K = 0.1$  in the ordinary liquid state.<sup>11</sup> According to a previous study of MTHF,<sup>12</sup> annealing the as-deposited film just above  $T_g$  resulted in a liquid with a significantly lower dielectric constant. While these cases of unusual liquids vary in how their states differ from the ordinary counterpart, a common feature is that these metastable states persist for a duration that is orders of magnitude longer than the primary structural relaxation time at the same temperature.

The aim of this study is to revisit the polyamorphism of vapor-deposited MTHF observed in a dielectric study by Riechers *et al.*<sup>12</sup> in more detail by broadband dielectric spectroscopy. To this end, MTHF is deposited onto interdigitated electrode (IDE) cells, which facilitate *in situ* monitoring of film growth and recording of the dielectric relaxation spectra in the  $10^{-2}$  Hz– $10^7$  Hz range. We find that vapor deposition of MTHF leads to a variety of metastable states that differ with respect to the loss profile and the peak relaxation frequency, with a qualitative difference between depositing below and above  $T_g = 91$  K.<sup>15</sup> Deposition onto a substrate at  $T = 0.82T_g$  gives rise to a supercooled liquid with somewhat faster relaxation dynamics relative to liquid-cooled MTHF and an additional slow process with Arrhenius-like temperature dependence of its time constant. Deposition at temperatures between  $1.3T_g$  and  $1.4T_g$  results in persistent states that display dielectric relaxation behavior between one and 1000 times faster than the ordinary liquid, with the factor depending on the deposition temperature and aging protocol. For instance, at  $T = 120$  K, where the structural relaxation time is  $\tau_\alpha < 1$  ns, it takes more than 1000 s for the liquid to recover the dynamics of bulk MTHF as obtained by cooling the liquid.

## II. EXPERIMENTAL

MTHF was purchased from Acros (99+%, stabilizer-free) and vapor-deposited as received in a home build setup described earlier.<sup>16</sup> Broadband dielectric spectra were taken with an Andeen–Hagerling ultraprecision bridge AH-2700A (100 Hz–20 kHz) and a Solartron SI-1260 (with transimpedance amplifier DM-1360 for frequencies  $10^{-2}$  Hz– $10^7$  Hz or DM-1370 for the  $10^{-2}$  Hz– $10^5$  Hz range). The sample environment was implemented in a closed-cycle helium cryostat (Leybold RDK 10-320) controlled by a Lakeshore Model 340 temperature controller using DT-470-CU sensors to facilitate adjustments in temperature between 30 K and 300 K. Most samples were deposited at  $0.82T_g$  [ $T_g(\text{MTHF}) = 91$  K<sup>15</sup>] or higher than  $1.3T_g$ . Reference dielectric spectra were recorded using a parallel plate capacitor with a diameter of 18 mm and 70  $\mu\text{m}$  electrode spacing.<sup>17</sup> The vapor-deposited samples were measured on an IDE cell, ABTECH IME 1050.5-FD-Au.<sup>18,19</sup> The IDE cell consists of 50 digit pairs on top of a 0.5 mm thick borosilicate glass substrate. Each digit has a width of  $w = 10$   $\mu\text{m}$  and a length of  $l = 5$  mm and is separated by  $s = 10$   $\mu\text{m}$  from its neighbors. The resulting periodicity is  $\lambda = 2(w + s) = 40$   $\mu\text{m}$ . Details regarding the setup and deposition process are described in a previous paper.<sup>12</sup> The desired MTHF deposition rate was controlled by the pressure of the MTHF reservoir ( $< 1$  mbar), which is connected to the deposition chamber via a needle valve and on/off valves.

To correct for the temperature difference between IDE surface and temperature sensor, all values were shifted uniformly by +2 K so that the loss peak of the experimental data after high-temperature deposition and annealing coincided with the loss peak position of reference data obtained for liquid-cooled (bulk) MTHF data measured in a parallel plate capacitor (see Fig. 1). This difference can be attributed to the sensor location on the back

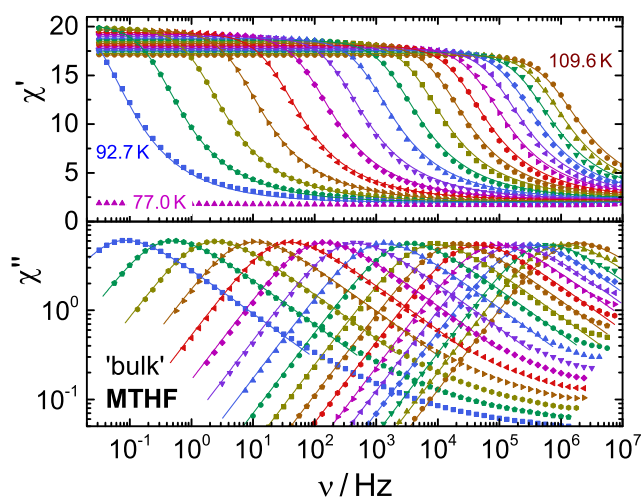


FIG. 1. Symbols represent temperature-dependent dielectric storage ( $\chi'$ ) and loss ( $\chi''$ ) spectra of melt-cooled MTHF measured in a parallel plate capacitor for temperatures from 109.6 K to 92.7 K in steps of 1 K and at 77.0 K. Lines are fits using the HN function in the peak region with temperature invariant shape parameters ( $\alpha = 0.91$  and  $\gamma = 0.55$ ).

side of the brass cell holder, the low thermal conductivity of the cell substrate, and the sample/vacuum interface being exposed to radiation.

Liquid 2-ethyl-1-hexanol (2E1H) was used as a calibration sample to determine the geometric capacitance,  $C_{\text{geo}}$ , where  $C_{\text{geo}}$  refers to the air/vacuum capacitor that can be filled with the sample material, i.e., excluding the substrate side. To this end, an ample amount of 2E1H was placed onto the cleaned cell at ambient temperature such that the IDE capacitor was filled completely, and the resulting capacitance increment was recorded. Based on the static dielectric constant of 2E1H at room temperature,  $\epsilon_s = 7.61$ ,<sup>20</sup> the geometric capacitance of the IDE was found to be  $C_{\text{geo}} = 2.15$  pF. To be able to determine the relation between the film thickness  $d$  and resulting susceptibility  $\chi_{\text{obs}}$ , an effective field height  $H$  of  $\lambda/8 = 5 \mu\text{m}$  was assumed,<sup>19</sup> with the proportionality being limited to  $d < 500$  nm.<sup>21,22</sup> It requires a film thickness of  $\lambda/2 = 20 \mu\text{m}$  to achieve complete filling of the capacitor volume. If the capacitor was filled completely with the material, the permittivity  $\epsilon^*$  on each side (deposition or substrate side) would be determined by the ratio  $\epsilon^* = C^*/C_{\text{geo}}$ , where  $C^*$  is the complex capacitance. For samples thinner than 500 nm, the relation that connects the incremental capacitance ( $\Delta C^*$ ) to the observed susceptibility ( $\chi_{\text{obs}}$ ) and the film thickness  $d$  is thus given by

$$\Delta C^*(\omega) = C_{\text{geo}}\chi_{\text{obs}}^*(\omega) = C_{\text{geo}}\chi^*(\omega) \cdot \varphi(d), \quad (1)$$

where  $\chi^*(\omega) = \epsilon^*(\omega) - 1$  denotes the reference data. The quantity  $\varphi(d)$  represents the thickness dependent filling factor, which is a monotonic function, but linear only for  $d < 500$  nm. In most cases, the IDE was filled beyond  $d = 500$  nm, and therefore, both  $\varphi$  and  $d$  were determined by comparing  $\Delta C^*$  of a partially filled IDE with a filling curve ( $\Delta C^*$  vs time at constant deposition rate) recorded to the point of a completely filled IDE capacitor.

All spectral line shapes were analyzed in terms of the empirical Havriliak–Negami (HN)<sup>23</sup> function,

$$\epsilon^*(\omega) = \epsilon_\infty + \frac{\Delta\epsilon}{(1 + (i\omega\tau_{\text{HN}})^\alpha)^\gamma}, \quad (2)$$

with  $\Delta\epsilon = \epsilon_s - \epsilon_\infty$ , where  $\epsilon_s$  and  $\epsilon_\infty$  are the permittivities in the limits of low and high frequencies, respectively. In this HN expression,  $\omega$  is the radian frequency,  $\tau_{\text{HN}}$  is a characteristic time constant, and  $\alpha$  and  $\gamma$  quantify the symmetric and asymmetric broadening, respectively. From these parameters, the peak time-constant can be determined:<sup>24</sup>

$$\tau_{\text{max}} = \tau_{\text{HN}} \sin^{-1/\alpha} \left( \frac{\alpha\pi}{2 + 2\gamma} \right) \sin^{1/\alpha} \left( \frac{\alpha\pi\gamma}{2 + 2\gamma} \right). \quad (3)$$

The dielectric susceptibility  $\chi^*(\omega)$  is derived from the measured complex capacities with ( $C_{\text{obs}}^*$ ) and without ( $C_{\text{empty}}^*$ ) sample using

$$\chi_{\text{obs}}^*(\omega) = \frac{C_{\text{obs}}^*(\omega) - C_{\text{empty}}^*(\omega)}{C_{\text{geo}}}. \quad (4)$$

Therefore, each sample measurement is subject to subtracting the data recorded for the empty IDE at the same temperature. This process eliminates the stray (parallel) capacitance from the measurement, which results from the borosilicate substrate side of the cell. Because adding a sample replaces vacuum with  $\epsilon = 1$  with  $\epsilon_{\text{obs}}^*$ , subtracting values for the empty IDE leads to  $\chi = \epsilon - 1$ .

### III. RESULTS

In order to obtain a reference dataset, MTHF was cooled from the melt and measured in a parallel plate capacitor. Figure 1 shows the real and imaginary part of the dielectric susceptibility spectra obtained between 110 K and 93 K and in the glassy state at 77 K. The spectra are consistent with literature data,<sup>25</sup> and can be described by HN fit functions with  $\alpha = 0.91$  and  $\gamma = 0.55$  at all temperatures when the excess-wing contribution is disregarded. The constant shape parameters imply that time–temperature superposition (TTS) is valid. The peak time constants follow a Vogel–Fulcher–Tammann (VFT) law,

$$\tau_{\text{max}} = \tau_0 \exp \left( \frac{B}{T - T_0} \right), \quad (5)$$

with parameters  $\tau_0 = 4 \times 10^{-16}$  s,  $B = 682$  K, and  $T_0 = 73.8$  K. These data will be used to compare PVD films against ordinary bulk MTHF prepared by cooling the melt, and this reference state will be designated as “bulk MTHF” in the following.

All subsequent results shown below are obtained by vapor deposition onto the IDE cell. The deposition conditions are characterized by the deposition temperature,  $T_{\text{dep}}$ , i.e., the substrate temperature during vapor deposition, and the deposition rate,  $r_{\text{dep}}$ , which is equal to the film thickness  $d$  divided by the deposition time,  $t_{\text{dep}}$ . Percentage filling factors are given in terms of the observed capacitance increment relative to the case of a completely filled IDE with  $d > 20 \mu\text{m}$ . Because  $\varphi(d)$  is not a linear function, these  $\varphi$  values are not equivalent to volume fraction. For MTHF, measurements aimed at observing the loss peak are limited by the available frequencies to a temperature range of about 92 K–100 K.

The results are presented in the following order: (1) experiments revisiting very thin films deposited at  $0.82T_g$ , as studied previously by Riechers *et al.*,<sup>12</sup> with the aim to illuminate the origin of the relaxation amplitude change that occurred at elevated temperatures, (2) results characterizing thicker films deposited at  $0.82T_g$ , and (3) experimental evidence for the unusual dynamics of films deposited at  $1.32T_g$  and beyond.

#### A. Very thin films

As previously reported,<sup>12</sup> a thin ( $\sim 100$  nm) film of MTHF deposited at 75 K is kinetically more stable than what is obtained by cooling the bulk liquid. When heating such a glass to more than 20 K above the glass transition temperature  $T_g$ , Riechers *et al.* observed a dielectric relaxation strength that is considerably reduced relative to the bulk liquid at the same temperature and reported a recovery of the state of bulk MTHF by annealing at an elevated temperature.<sup>12</sup> This interpretation was based on the observed change in the overall relaxation strength. These earlier experiments were

performed at a fixed frequency of 1 kHz and during temperature scans.

For a more in-depth analysis, this work provides the entire dielectric spectra, as shown in Fig. 2. Two sets of spectra taken at temperatures between 92 K and 98 K are shown: one measured directly after deposition and a second set measured after heating the sample to 120 K ( $=T_g + 29$  K). The spectra of the second run can be scaled to those of the first run, implying that both  $\chi_s$  and  $\chi_\infty$  differ by the same factor of around 0.7. If the annealing-induced change in the relaxation strength,  $\Delta\epsilon$ , was the result of a different liquid state,  $\chi_\infty$  would not have increased in the same manner. Based on this frequency invariant scaling behavior, a realistic rationale is that the amount of liquid filling the capacitor has changed. This could be the result of a preference of MTHF to reside on the borosilicate glass surface rather than on top of the gold electrode fingers. The material situated between the gold fingers generates much more dielectric signal than on top of the gold surface, but it requires sufficient fluidity for the sample to be able to move from a uniform (as-deposited) layer to selectively avoid the gold surface contact. Thus, while the relaxation strength of this state is indeed reduced in comparison to bulk MTHF, the difference between the first and second sets of spectra is attributed to a mere re-allocation of the sample material on the IDE and not to a change of the material's state itself, in contrast to the interpretation given by Riechers *et al.* This apparent change in the dielectric amplitude is diminished for thicker films, and layers with  $d = 250$  nm or more show no such amplitude increase after heating to 120 K. Accordingly, all results shown below are not susceptible to this apparent amplitude effect.

## B. Films deposited below $T_g$

MTHF in an ultrastable state was prepared by depositing the material on the IDE cell at  $T_{\text{dep}} = 75$  K ( $= 0.82T_g$ ) until filled to

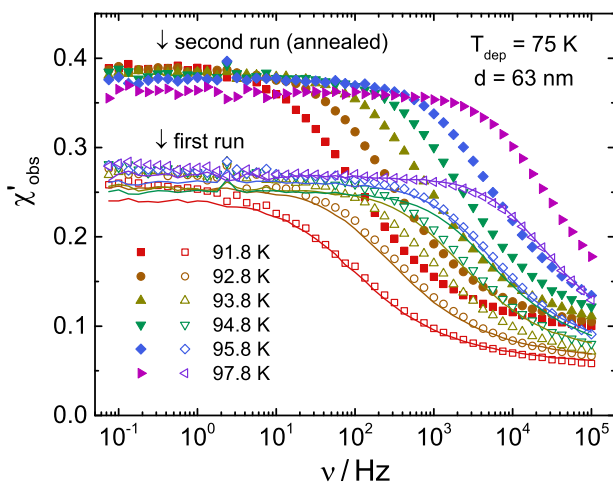


**FIG. 2.** Temperature dependent dielectric spectra of a 63 nm thick kinetically stable MTHF film deposited at  $T_{\text{dep}} = 75$  K with a rate of  $r_{\text{dep}} = 0.19$  nm/s for  $t_{\text{dep}} = 320$  s. Open symbols (first run) are taken directly after deposition and full symbols (second run) are recorded after annealing at 120 K. Both sets of curves are recorded in the order from low to high temperature to mimic the protocol of Riechers *et al.*<sup>12</sup> Lines reflect the second run data after scaling down by a factor of about 0.7.

$\phi = 68\%$ , corresponding to a film thickness of about  $d = 10$   $\mu\text{m}$ . The deposition rate was determined to be  $r_{\text{dep}} = 0.21$  nm/s, equivalent to  $t_{\text{dep}} = 38\,000$  s. The dielectric susceptibility spectra of this film are shown in Fig. 3 for the as-deposited glass at  $T = 75$  K and for the liquid state between 91 K and 104 K.

Surprisingly, for a molecular glassformer, the spectrum reveals not only the typical main peak with excess wing but also a separate peak at lower frequencies with an amplitude of  $\sim 10\%$  of the total relaxation strength. The main relaxation peak is described by a HN fit function, with an increase in broadening of this peak with the decrease in temperature, as demonstrated by the HN shape parameters  $\alpha$  and  $\gamma$  in Fig. 4. These spectra show loss profiles similar to those of bulk MTHF at higher temperatures, but all peak frequencies,  $\nu_{\text{max}}$ , are about a decade higher than those of bulk MTHF at the same temperature. Furthermore, the main peaks do not show the typical low frequency power law behavior with slope  $\alpha = +1$  in a  $\log \epsilon''$  vs  $\log \omega$  plot. Instead, the main relaxation peak is more symmetrically broadened at lower temperatures and thus described by a symmetric HN fit function with constant shape parameters  $\alpha = 0.65$  and  $\gamma = 1$ . It is remarkable that the slower process has a much weaker temperature dependence of its time constant than the main peak. Above 102 K, crystallization starts to decrease the total relaxation strength, but apart from the amplitudes, the overall spectral shape appears to be unaffected. This homogeneous decrease indicates that both relaxation peaks are affected equally by the reduction in the liquid volume fraction due to crystallization.

To examine the influence of the deposition rate, an equally thick but more rapidly ( $r_{\text{dep}} = 17.3$  nm/s and  $t_{\text{dep}} = 450$  s) deposited sample was prepared at  $T_{\text{dep}} = 75$  K. The inset of Fig. 5 shows the film growth for slow and fast deposition, i.e., capacitance increase,

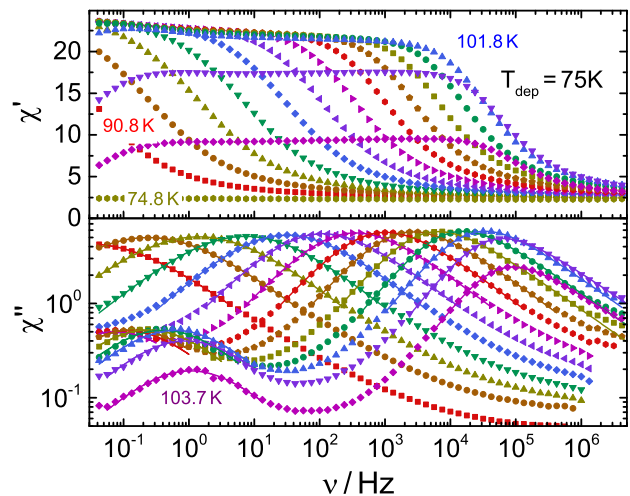


**FIG. 3.** Temperature-dependent dielectric susceptibility spectra of MTHF deposited at  $T_{\text{dep}} = 75$  K with a rate of  $r_{\text{dep}} = 0.21$  nm/s for  $t_{\text{dep}} = 38\,000$  s, resulting in a film thickness  $d = 8.0$   $\mu\text{m}$ . Lines are fits to the individual peak regions using separate HN functions: one for the slow process with  $\alpha = 0.65$  and  $\gamma = 1$  and one for the  $\alpha$  process with shape parameters shown in Fig. 4. For the two highest temperatures, the overall amplitude reduction and descent of  $\chi'$  at low frequencies are due to crystallization.

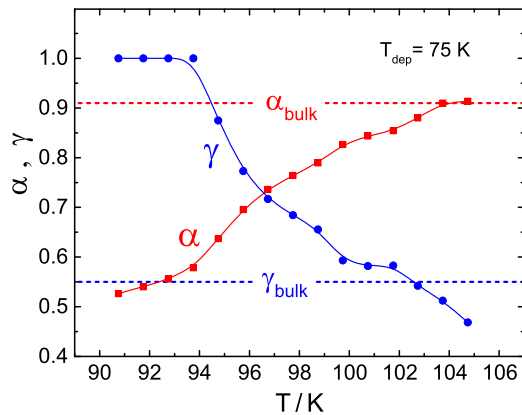


**FIG. 4.** Temperature-dependent HN fit parameters  $\alpha$  and  $\gamma$  (symbols) of the main dielectric peak for the measurements shown in Fig. 3. Solid lines are guides only. The dashed lines represent the temperature invariant parameters for bulk MTHF.

$\Delta C$ , vs relative deposition time,  $t/t_{\text{dep}}$ . After normalization to  $t_{\text{dep}}$ , the curves superimpose despite their rates  $r_{\text{dep}}$  differing by factor of 84. As shown in Fig. 5, the relaxation strength in the case of faster deposition is nearly the same as the one obtained with slow deposition. It is interesting to note that the separate slow process does not appear for the sample deposited at the higher rate. The spectral shape of the fast deposited MTHF can be approximated by HN fits with the temperature invariant parameters  $\alpha = 0.91$  and  $\gamma = 0.55$  (see Fig. 5), the values matching those obtained for bulk MTHF spectra. Within the obtainable resolution, the dielectric constants of these

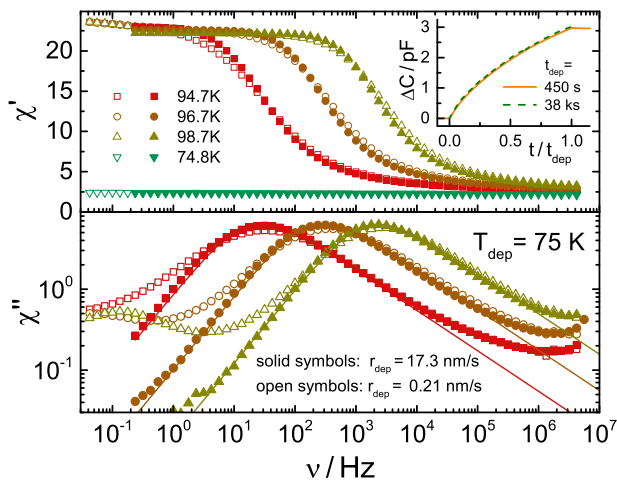


**FIG. 5.** Dielectric susceptibility spectra of MTHF, vapor-deposited at  $T_{\text{dep}} = 75$  K, using two different deposition rates to achieve films with about  $d = 10 \mu\text{m}$  thickness: a low rate with  $r_{\text{dep}} = 0.21$  nm/s and  $t_{\text{dep}} = 38000$  s (open symbols, data of Fig. 3) and a high rate with  $r_{\text{dep}} = 17.3$  nm/s and  $t_{\text{dep}} = 450$  s (solid symbols). The additional slow process near 0.1 Hz appears only with the low deposition rate. Data from the fast deposition are described by bulk-like HN parameters, i.e.,  $\alpha = 0.91$  and  $\gamma = 0.55$  (see lines). The inset shows the increase in capacity during deposition for both cases on a reduced time axis.

films also match those of the bulk supercooled MTHF. Regardless of the bulk-like loss profiles, the relaxation times of these films remain about a factor of 10 below those of ordinary MTHF at the same temperature.

To check if the state obtained by slow deposition can be transformed into that achieved by fast deposition via annealing at elevated temperatures, a thinner layer of  $d = 250$  nm was deposited to avoid crystallization. This sample was slowly deposited ( $r_{\text{dep}} = 0.25$  nm/s; see the inset of Fig. 6) at  $T_{\text{dep}} = 75$  K and directly measured at that temperature. A second spectrum is recorded at 98 K, which shows the same shape as the slowly deposited MTHF depicted in Fig. 5. Interestingly, when repeating the measurement at  $T = 98$  K after briefly heating the sample to 120 K, the observed spectrum resembles that of the fast deposited sample, with the same static dielectric constant  $\chi_s$ . Cooling back down to 75 K reveals that the plateau value,  $\chi_\infty$ , has increased relative to the as-deposited level. Presumably, the annealing erases the ultrastable features of the film, such as the suppression of secondary relaxations in as-deposited stable glasses, as reported earlier.<sup>12</sup> Reheating to 98 K results in the same spectra as measured directly after annealing and confirms the high stability of the phase even when measured many Kelvins above  $T_g$ . Overall, fast deposition and high temperatures will affect the additional slow process present in films deposited at  $T_{\text{dep}} = 75$  K, but the loss peak frequency of the main process remains a decade higher than that of bulk MTHF. When attempting to anneal such films at temperatures exceeding 120 K, or for longer times at 120 K, the samples crystallized.

### C. Films deposited above $T_g$

According to the results presented in Subsection III B, the peak dielectric loss frequencies of films deposited at  $T_{\text{dep}} = 75$  K are about one decade above those of bulk MTHF prepared by cooling the melt. This unusual feature remains even after annealing at 120 K, where

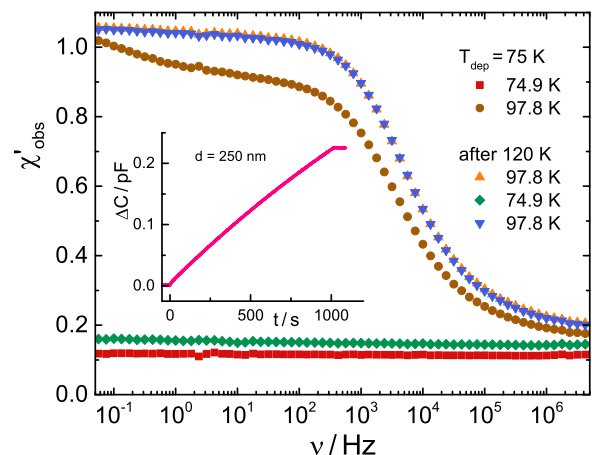


**FIG. 6.** Spectra of the real part of dielectric susceptibility of MTHF for a 250 nm thick film deposited slowly at  $T_{\text{dep}} = 75$  K with  $r_{\text{dep}} = 0.25$  nm/s and  $t_{\text{dep}} = 1015$  s. Data are measured directly after deposition and again after annealing at 120 K, as indicated in the legend. The inset shows the linear increase in capacity during deposition.

the structural relaxation time is  $\tau_\alpha < 1$  ns. Therefore, the following question arises: under which circumstances can the behavior of ordinary MTHF be recovered after vapor deposition? Considering the previous result that the behavior of vapor deposited MTHF does more closely resemble that of its bulk counterpart when employing high deposition temperatures and deposition rates, we chose  $T_{\text{dep}} = 120$  K and  $r_{\text{dep}} = 138$  nm/s with  $t_{\text{dep}} = 70$  s for a subsequent experiment, leading to a filling factor  $\varphi = 91\%$ . Additionally, the sample was held at  $T_{\text{dep}}$  for a waiting time  $t_{\text{wait}} = 1500$  s before cooling down to temperatures between 99 K and 92 K at which the loss peak falls within the experimental frequency window. The resulting spectra are depicted in Fig. 7 and coincide very accurately in shape, amplitude, and time constant with the reference parallel plate capacitor measurements of bulk MTHF shown in Fig. 1.

A reduction in the waiting time at  $T_{\text{dep}}$  can lead to very different results. This is demonstrated in Fig. 8 for a sample that was deposited at  $T_{\text{dep}} = 120$  K at a rate of  $r_{\text{dep}} = 146$  nm/s for  $t_{\text{dep}} = 70$  s ( $\varphi = 90\%$ ), but with a shorter waiting time of  $t_{\text{wait}} = 275$  s relative to the case of Fig. 7. Surprisingly, these spectra in Fig. 8 are symmetrically broadened and poorly described by a single HN curve, with the deviations from HN behavior being more pronounced at lower temperatures. The inset of Fig. 8 shows the HN fit parameters  $\alpha$  and  $\gamma$  strongly changing with temperature, in contrast to the TTS behavior of bulk MTHF. More importantly, the loss peak frequencies indicate dynamics that are three decades faster than expected from bulk MTHF cooled from the melt.

Interestingly, the loss peak of MTHF films observed at 95 K can assume frequency positions between these two extremes (bulk-like or three decades higher) when varying the deposition temperature between 120 K and 127 K, the deposition rate between 26 nm/s and 146 nm/s (equivalent to deposition times between 650 s and 70 s),

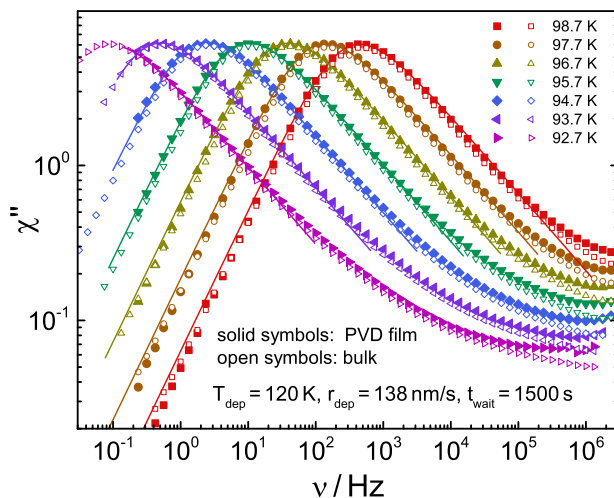


**FIG. 7.** Dielectric loss spectra of MTHF deposited at  $T_{\text{dep}} = 120$  K with a high deposition rate ( $r_{\text{dep}} = 138$  nm/s and  $t_{\text{dep}} = 70$  s) and long waiting time ( $t_{\text{wait}} = 1500$  s) at  $T_{\text{dep}}$  (solid symbols). The rise of  $\chi''$  at high frequencies is considered an artifact due to imperfect substrate corrections. The lines represent HN fits. For a comparison, bulk MTHF data at the same respective temperatures are included as open symbols.

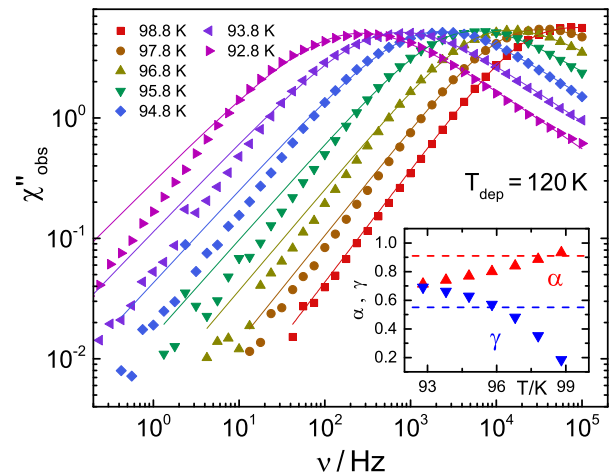


**FIG. 8.** Temperature-dependent dielectric loss spectra of MTHF (symbols) measured after fast deposition at  $T_{\text{dep}} = 120$  K, using  $r_{\text{dep}} = 146$  nm/s and  $t_{\text{dep}} = 70$  s, and an additional waiting time  $t_{\text{wait}} = 275$  s at  $T_{\text{dep}}$ . The resulting film thickness is  $d = 10.2$   $\mu\text{m}$ . The HN fit lines deviate from the measurement due to the bimodal broadening of the spectra. At  $T = 95$  K, the peak frequency is three decades above that of the bulk material at the same temperature, as shown in Fig. 1. The inset shows the HN parameters vs temperature, which are incompatible with TTS. The dashed lines mark the HN parameters obtained for bulk MTHF.

and the waiting time between 0 s and 1500 s (see Fig. 9 and Table I). Note that there is a  $<10\%$  deviation of static susceptibilities in Fig. 9, and due to the correlation of  $\chi_s$  with  $\chi_\infty$ , it is judged that this is the result of the cell calibration rather than a true change in the relaxation strength. Once the temperature of these films is below

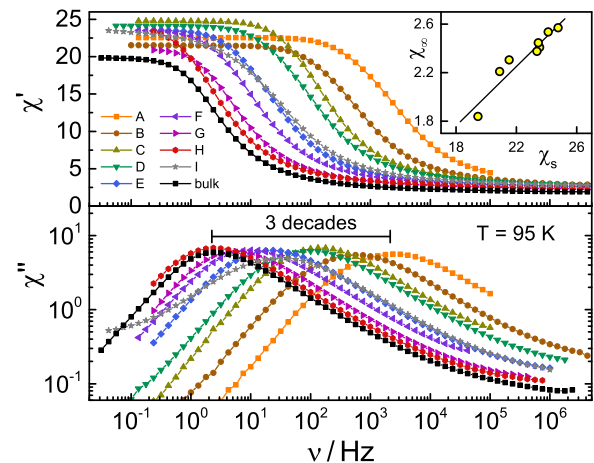


**FIG. 9.** Comparison of dielectric susceptibility spectra of MTHF, all taken at  $T = 95$  K, deposited at various temperatures, deposition rates, and waiting times, as indicated in the legend. The resulting spectra cover a broad range of peak frequencies (3 decades) and differ in peak widths. The amplitudes are normalized to the respective filling factors  $\varphi$ . Film thicknesses are in the range from  $d = 8$   $\mu\text{m}$  to 24  $\mu\text{m}$ . Black squares show data for bulk MTHF measured in a parallel plate capacitor. The deposition parameters for samples A–I are compiled in Table I. The inset shows the correlation between  $\chi_\infty$  and  $\chi_s$  for samples A–H.

**TABLE I.** Overview of the deposited samples for which dielectric spectra are shown, including  $T_{\text{dep}}$ ,  $r_{\text{dep}}$ ,  $t_{\text{dep}}$ ,  $t_{\text{wait}}$ , and filling factor  $\varphi$  of the capacitors.

Sample	$T_{\text{dep}}$ (K <sup>-1</sup> )	$r_{\text{dep}}$ (nm <sup>-1</sup> s <sup>-1</sup> )	$t_{\text{dep}}$ (s <sup>-1</sup> )	$t_{\text{wait}}$ (s <sup>-1</sup> )	$\varphi$ (%)
A	120	145.6	70	275	91
B	120	33.2	500	0	88
C	124	114.4	100	100	91
D	120	105.8	170	40	97
E	125	25.96	650	1400	92
F	120	107.9	225	215	100
G	127	27.18	610	1300	95
H	120	137.9	70	1500	90
I	73	0.21	38 000	0	68

100 K, the loss peak position for these states is time invariant for hours. Even longer persistence times have been observed, but crystallization is a limiting factor.

#### IV. DISCUSSION

Since the discovery of high kinetic stability via PVD techniques with suitable deposition parameters,<sup>26</sup> many organic molecular glass formers have been subject to PVD studies, including MTHF by Riechers *et al.*<sup>12</sup> In that study, it was concluded that a film of MTHF deposited near  $T_{\text{dep}} = 75$  K does not transform into the same state reached by cooling the melt when heated to just above  $T_g$ . This observation of distinct metastable states with distinguishable dynamics is indicative of two different amorphous structures and thus polymorphism. This interpretation is confirmed by the findings presented here. However, based on the relaxation amplitude increase when approaching 120 K, Riechers *et al.* also concluded that the liquid converts to the ordinary state of MTHF with the same properties that would be obtained from cooling the melt. From the present experiments, it becomes evident that this amplitude increase is due to the rearrangement of the material on the surface of the IDE cell. The driving force is the ability of very thin films to minimize their free energy by residing preferentially on the borosilicate substrate, rather than on the gold surface. This change in sample topology requires macroscopic flow and thus sets in only at temperatures considerably above  $T_g$ . Consequently, the apparent amplitude increase observed earlier should not have been interpreted as conversion to the ordinary bulk state. Summarizing the discussion of and comparison to the previous findings by Riechers *et al.*, all previous observations regarding vapor deposited MTHF are consistent with the present results, with the exception of the interpretation of the increase in absolute relaxation amplitudes due to annealing at  $1.3T_g$ .

Films deposited at  $T_{\text{dep}} = 75$  K ( $=0.82T_g$ ) display a reduced value of  $\chi_\infty$  in the as-deposited glassy state (see Fig. 6), as reported in more detail previously.<sup>12</sup> Measuring such slowly deposited and kinetically stable films in the 92 K–99 K temperature range reveals two distinct relaxation processes: first, a main loss peak with a reproducible peak position, which is about one decade higher in frequency relative to bulk MTHF (see Fig. 10). Its loss profile differs

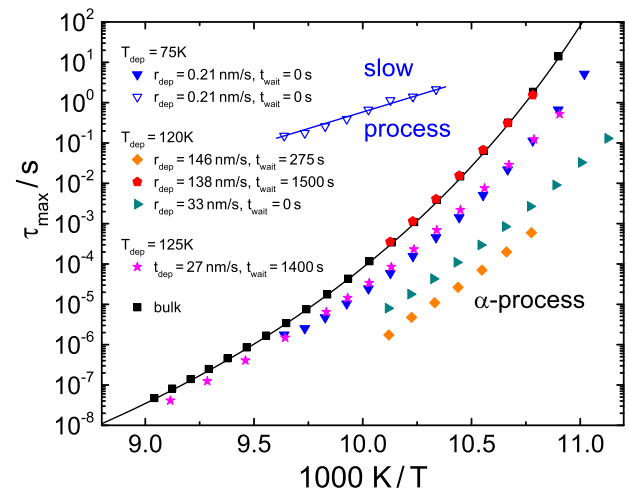


**FIG. 10.** Peak dielectric relaxation times vs inverse temperature for the main relaxation peak of bulk MTHF (black squares) with the corresponding VFT fit (black line) and for vapor deposited films with various deposition conditions listed in the legend. Open symbols show the additional slow process that occurs with  $T_{\text{dep}} = 75$  K, with activation energy  $\Delta E = 0.35$  eV.

qualitatively from that of bulk MTHF, and the temperature dependence of its  $\tau_{\text{max}}$  follows a VFT law with lower fragility parameter. Second, these spectra show another dielectric process with a peak frequency positioned between four and five decades below that of the main peak (see Fig. 3), with about 10% of the total relaxation amplitude and an Arrhenius-like temperature dependence of its  $\tau_{\text{max}}$ . The total dielectric relaxation amplitude is similar to that of the bulk state, but the dynamics of this metastable state differ qualitatively from bulk MTHF behavior. Annealing these films at 120 K eliminates the slow peak without changing the static dielectric constant (see Fig. 6), implying that the amplitude of the slow peak has shifted into the main  $\alpha$ -process by annealing. Note that the drop of  $\chi'$  near 0.2 Hz for the  $T = 97.8$  K ( $T_{\text{dep}} = 75$  K) curve is the signature of the extra slow process, as shown in Fig. 5. Attempts to anneal at a higher temperature or for a longer duration always led to crystallization rather than conversion to the bulk MTHF state. Depositing at a high rate has an effect similar to that of annealing (see Fig. 5). The observation that the appearance of the additional slow peak is tied to slow deposition at  $T_{\text{dep}}$  below  $T_g$  might suggest a correlation with the formation of a glass of high kinetic stability. As the slow peak also occurs for  $T_{\text{dep}} = 40$  K, where the signature of stability is less pronounced,<sup>12</sup> the cause for the slow peak may not be connected to high kinetic stability itself.

The deposition of MTHF at or above 120 K, i.e., at  $T_{\text{dep}} > 1.32T_g$ , leads to films very different from those obtained with  $T_{\text{dep}} < T_g$  as well as from bulk MTHF. At  $T = 120$  K, only 17 K below the melting temperature, the dielectric relaxation time of MTHF is about 1 ns or faster, leading to the expectation that MTHF should be able to relax quickly to the ordinary supercooled state. Instead, these films show considerable deviations from bulk-like dynamics, which

persist for times that are many orders of magnitude above the dielectric relaxation time. The main signature of these deviations is a continuum of different time constants across more than three decades when measured at  $T = 95$  K. In Fig. 9, this is signified by a variation of  $\nu_{\max}$  between 2 Hz and 2 kHz, while  $\nu_{\max} = 2$  Hz for bulk MTHF. These curves indicate that the peak position is a matter of the deposition temperature (120 K–127 K), the deposition rate (26 nm/s–146 nm/s), and the waiting time (0 s–1500 s) at  $T_{\text{dep}}$ . The systematic effects of these parameters on  $\nu_{\max}$  are as follows: (1) higher deposition temperatures lead to lower  $\nu_{\max}$  values, (2) higher deposition rates lead to lower  $\nu_{\max}$  values, and (3) increased total times ( $t_{\text{dep}} + t_{\text{wait}}$ ) spent at  $T_{\text{dep}}$  result in significant shifts of  $\nu_{\max}$  to lower frequencies, i.e., to a stronger resemblance to the properties of bulk MTHF. It can also be observed that the loss profile deviates more strongly from that of bulk MTHF as the peak frequency is increased beyond the  $\nu_{\max} = 2$  Hz value of the bulk state. Interestingly, these states are metastable for several hours or more, regardless of how much higher the actual peak frequency is compared to the bulk value of 2 Hz at 95 K.

Among the dielectric spectra shown in Fig. 9, the state associated with the lowest peak frequency (2 Hz, red circles) coincides with the reference measurements of bulk MTHF (black squares) in terms of the time-constant, spectral shape, TTS behavior, and relaxation strength. This validates the calculation of the susceptibilities and the normalization to the filling factor. More importantly, this agreement demonstrates that the unusual state of MTHF with fast dynamics can eventually be transformed to the ordinary state, i.e., the one obtained by cooling the melt. This gradual transformation, which shifts  $\nu_{\max}$  by three decades, could not be observed in real time because for  $T > 120$  K, the peak is outside the available frequency window. Regardless, the transformation appears to occur as a continuous slowing down of dynamics rather than via a change in the population of two distinct states. In the case of a two state transformation, an isosbestic point should appear in Fig. 9 at around 100 Hz.

The temperature dependent peak time constants of MTHF are compiled in Fig. 10. The bulk case (black squares) can be described by a VFT temperature dependence (black line). Near  $T_g$ , the  $\tau_{\max}$  value for MTHF deposited at 75 K is one decade lower than that of bulk MTHF but approaches the bulk time constants at high temperatures. The slow process with an Arrhenius temperature dependence (open symbols,  $\Delta E = 0.35$  eV), which arises for  $T_{\text{dep}} = 75$  K and low  $r_{\text{dep}}$  prior to annealing, appears at relaxation times at least four decades higher than the main peak. For samples deposited at  $T_{\text{dep}} = 120$  K or above, the curvature in this activation graph becomes less pronounced, as the system is trapped in a state with faster dynamics. Eventually, the temperature dependence becomes practically Arrhenius-like with  $\Delta E = 0.77$  eV for the sample with the shortest relaxation times. Thus, it appears that states of vapor deposited MTHF with faster dynamics are subject to lower fragilities, if judged by the extent of curvature in Fig. 10.

Obviously, the PVD process facilitates capturing MTHF in at least three metastable states: those with one or two relaxation processes when deposited at  $T_{\text{dep}} < T_g$  and one obtained with  $T_{\text{dep}} < T_g$  showing dynamics that are up to three decades faster than the bulk counterpart. It seems reasonable to assume that different dynamics are linked to distinguishable structures. All three cases differ from

what is known from studies in which the sample is prepared by cooling the melt, which invariably leads to spectra such as those of Fig. 1. For the unusual states observed here, the high kinetic stability that can be achieved by PVD preparation can be a relevant factor only for glasses deposited below  $T_g$ . Since kinetic stability is not the sole cause for the formation of alternative amorphous states, it remains to clarify which features inherent in physical vapor deposition lead to polyamorphic states. Other PVD specific features which might serve as the cause of these phenomena include the high effective cooling rates associated with PVD, molecules equilibrating at the surface rather than in the bulk, and the possible introduction of anisotropy in the films. Structural information from scattering experiments is required to better characterize these different states. In the absence of such data, we can only speculate on the structural features that could lead to the range of dynamics observed here. Options to be considered are plastic crystal states and the role of weak hydrogen bonding.

Plastic crystals are condensed phases with crystal-like positions of molecules and thus high translational symmetry, but retain the reorientational degrees of freedom of the liquid state.<sup>7</sup> In cases such as those of ethanol, where both the liquid and plastic crystal states can be compared, dielectric relaxation amplitudes are similar, but the time constants differ by one to two decades and are subject to different activation parameters.<sup>7,27</sup> The main dielectric peak of MTHF vapor deposited at  $T_{\text{dep}} = 75$  K would be consistent with the dielectric behavior expected of plastic crystals, i.e., relaxation spectra similar to those of supercooled liquids but with altered time constants.<sup>7</sup>

As a potential explanation for the states obtained by depositing at  $T_{\text{dep}} > 120$  K, we consider the role of hydrogen bonding. Given the chemical structure of MTHF, the only intermolecular interactions are of van der Waals (vdW) type and weak CH...O H-bonds.<sup>28</sup> In this regard, we note that the boiling point of MTHF ( $T_b = 353$  K<sup>29</sup>) is 8 K higher than that of methyl-cyclopentane (MCP,  $T_b = 345$  K<sup>30</sup>), despite MTHF being nearly of the same weight, shape, and size. A third structurally similar molecule is 2-methylpyrrolidine (MP,  $T_b = 372$  K<sup>31</sup>), exhibiting a boiling temperature that is 19 K higher than that of MTHF. Comparing the molecular structures, the oxygen of MTHF is replaced by an NH-group in MP, which acts as a slightly weaker H-bond acceptor than oxygen, but does introduce a donor into the system. Therefore, the attractive interactions in MP are increased compared to MTHF. The strength of a CH...O H-bridge, approximately twice as strong as van der Waals bonds, is between those of the classic OH...O H- and vdW-bonds. Therefore, we conclude that a significant influence on molecular interactions in (vapor deposited) MTHF can be introduced by weak H-bonds. Compared with  $k_B T$  under ambient conditions, the thermal energy at temperatures near the glass transition of MTHF is very low, and thus, even weak H-bonds could affect the structure of vapor deposited MTHF. If this reasoning holds, other systems with weak H-bonds and low  $T_g$  are potential candidates for similar phenomena. Systems subject to H-bonding such as monohydroxy alcohols are dominated by H-bonds below 250 K<sup>32</sup> and usually have much higher glass transition temperatures. The relatively low thermal energy at or below the  $T_g$  of MTHF promotes the influence of H-bonds, possibly introducing supramolecular structures with low free energies. Such structures emerging from H-bonding would not lead to strong orientational correlation since the dipole moment has no strong correlation to the

H-bond direction. As a source for the unusual dynamics obtained by depositing at  $T_{\text{dep}} > 120$  K, this is consistent with our observation that there is no strong change in relaxation strength, which is equivalent to the Kirkwood factor remaining close to unity. Such a picture based on H-bond effects may also be compatible with the continuous rather than two-state transition to bulk behavior via annealing.

Previous molecular dynamics (MD) simulations have provided considerable insight into the details of physical vapor deposition. Specifically, the role of the mobile surface layer has been identified for the case of trehalose.<sup>33</sup> Moreover, the MD simulation reveals the anisotropy of PVD films,<sup>13</sup> which have been observed experimentally. In the context of MTHF, the MD simulation could yield answers to the origin of the unusual state obtained by deposition at 120 K, where structural relaxation times are  $< 1$  ns. Because these small time constants are within reach of MD techniques, simulations should be able to observe the equilibrium structure and dynamics of such PVD films.

## V. SUMMARY AND CONCLUSION

We have conducted a broadband dielectric relaxation study on vapor deposited films of MTHF ( $T_g = 91$  K) for various deposition temperatures, deposition rates, and annealing conditions. Slow deposition with  $T_{\text{dep}} = 0.82 T_g = 75$  K leads to a glass with high kinetic stability, and transforming this glass to a state with reorientational dynamics above  $T_g$  reveals two dielectric relaxation features: a primary loss peak indicating dynamics that are a decade faster than those of bulk MTHF and an additional weak process with 10% of the total amplitude and a loss peak position that is at least four frequency decades below the main peak. This slower process disappears upon annealing at 120 K and does not occur when preparing the sample at a higher deposition rate. More extensive annealing leads to crystallization of these films rather than converting to the bulk MTHF state. Deposition at  $T_{\text{dep}} > 1.32 T_g = 120$  K, where the structural relaxation time of bulk MTHF is  $< 1$  ns, results in a state with a single dielectric relaxation process with a peak frequency position that is three decades above that of bulk MTHF prepared by cooling the melt to 95 K. Annealing for at least 1000 s at 120 K is required to recover the dynamics of bulk MTHF. Less efficient annealing leads to a quasi-continuum of peak frequencies between one and 1000 times higher than the bulk counterpart.

Whenever the dielectric loss peak frequency does not match the bulk value at the same temperature, the loss profile and the temperature dependence are not the same as the bulk behavior. This is common to all deposition conditions. Also common to all states is that their dynamics in the 91 K–99 K range, i.e., above  $T_g$ , do not change for hours or days. Because we observe multiple distinct liquid states with long-lived metastability, MTHF satisfies our definition of polyamorphism when prepared by PVD techniques. This is similar to the previous observations of polyamorphism observed in the context of PVD,<sup>9–12</sup> where temperatures far exceeding  $T_g$  can be required for a conversion to the ordinary supercooled state. As potential explanations regarding the origin of these unusual dynamics and thus structures of MTHF, plastic crystal phases and the role of hydrogen bonding are

discussed. However, a more rigorous and complete understanding of vapor deposited MTHF requires further experiments determining the density, structure, and thermal behavior of such films obtained by PVD.

## ACKNOWLEDGMENTS

This work was supported by the National Science Foundation under Grant No. CHE-1854930.

## DATA AVAILABILITY

The data that support the findings of this study are available from the corresponding author upon reasonable request.

## REFERENCES

- 1 H. Tanaka, "Liquid–liquid transition and polyamorphism," *J. Chem. Phys.* **153**, 130901 (2020).
- 2 A. Ha, I. Cohen, X. Zhao, M. Lee, and D. Kivelson, "Supercooled liquids and polyamorphism," *J. Phys. Chem.* **100**, 1–4 (1996).
- 3 W. Tang and J. H. Perepezko, "Polyamorphism and liquid–liquid transformations in d-mannitol," *J. Chem. Phys.* **149**, 074505 (2018).
- 4 M. Zhu, J.-Q. Wang, J. H. Perepezko, and L. Yu, "Possible existence of two amorphous phases of d-mannitol related by a first-order transition," *J. Chem. Phys.* **142**, 244504 (2015).
- 5 M. Zhu and L. Yu, "Polyamorphism of D-mannitol," *J. Chem. Phys.* **146**, 244503 (2017).
- 6 R. Kurita and H. Tanaka, "On the abundance and general nature of the liquid–liquid phase transition in molecular systems," *J. Phys.: Condens. Matter* **17**, L293–L302 (2005).
- 7 R. Brand, P. Lunkenheimer, and A. Loidl, "Relaxation dynamics in plastic crystals," *J. Chem. Phys.* **116**, 10386–10401 (2002).
- 8 M. Götz, T. Bauer, P. Lunkenheimer, and A. Loidl, "Supercooled-liquid and plastic-crystalline state in succinonitrile-glutaronitrile mixtures," *J. Chem. Phys.* **140**, 094504 (2014).
- 9 S. Capponi, S. Napolitano, N. R. Behrnd, G. Couderc, J. Hulliger, and M. Wübbenhorst, "Structural relaxation in nanometer thin layers of glycerol," *J. Phys. Chem. C* **114**, 16696–16699 (2010).
- 10 S. Capponi, S. Napolitano, and M. Wübbenhorst, "Supercooled liquids with enhanced orientational order," *Nat. Commun.* **3**, 1233 (2012).
- 11 A. R. Young-Gonzales, A. Guiseppi-Elie, M. D. Ediger, and R. Richert, "Modifying hydrogen-bonded structures by physical vapor deposition: 4-methyl-3-heptanol," *J. Chem. Phys.* **147**, 194504 (2017).
- 12 B. Riechers, A. Guiseppi-Elie, M. D. Ediger, and R. Richert, "Ultrastable and polyamorphic states of vapor-deposited 2-methyltetrahydrofuran," *J. Chem. Phys.* **150**, 214502 (2019).
- 13 M. D. Ediger, J. de Pablo, and L. Yu, "Anisotropic vapor-deposited glasses: Hybrid organic solids," *Acc. Chem. Res.* **52**, 407–414 (2019).
- 14 W. Dannhauser, "Dielectric study of intermolecular association in isomeric octyl alcohols," *J. Chem. Phys.* **48**, 1911–1917 (1968).
- 15 R. Richert and C. A. Angell, "Dynamics of glass-forming liquids. V. On the link between molecular dynamics and configurational entropy," *J. Chem. Phys.* **108**, 9016–9026 (1998).
- 16 H. B. Yu, M. Tyllinski, A. Guiseppi-Elie, M. D. Ediger, and R. Richert, "Suppression of  $\beta$  relaxation in vapor-deposited ultrastable glasses," *Phys. Rev. Lett.* **115**, 185501 (2015).
- 17 H. Wagner and R. Richert, "Equilibrium and non-equilibrium type  $\beta$ -relaxations: D-sorbitol versus *o*-terphenyl," *J. Phys. Chem. B* **103**, 4071–4077 (1999).
- 18 L. Yang, A. Guiseppi-Wilson, and A. Guiseppi-Elie, "Design considerations in the use of interdigitated microsensor electrode arrays (IMES) for impedimetric characterization of biomimetic hydrogels," *Biomed. Microdevices* **13**, 279–289 (2011).

- <sup>19</sup>W. Olthuis, W. Streekstra, and P. Bergveld, "Theoretical and experimental determination of cell constants of planar-interdigitated electrolyte conductivity sensors," *Sens. Actuators, B* **24**, 252–256 (1995).
- <sup>20</sup>A. Ghanadzadeh Gilani, H. Ghanadzadeh, K. Bahrpaima, and A. Ranjkesh, "Dielectric properties of binary mixtures of three butanediols with 1, 4-dioxane and 2-ethyl-1-hexanol at  $t = 298.2$  K," *J. Chem. Thermodyn.* **42**, 967–972 (2010).
- <sup>21</sup>A. Sepúlveda, M. Tylinski, A. Guiseppi-Elie, R. Richert, and M. D. Ediger, "Role of fragility in the formation of highly stable organic glasses," *Phys. Rev. Lett.* **113**, 045901 (2014).
- <sup>22</sup>E. Thoms, J. P. Gabriel, A. Guiseppi-Elie, M. D. Ediger, and R. Richert, "In situ observation of fast surface dynamics during the vapor-deposition of a stable organic glass," *Soft Matter* **16**, 10860 (2020).
- <sup>23</sup>S. Havriliak and S. Negami, "A complex plane representation of dielectric and mechanical relaxation processes in some polymers," *Polymer* **8**, 161–210 (1967).
- <sup>24</sup>R. Richert, F. Stickel, R. S. Fee, and M. Maroncelli, "Solvation dynamics and the dielectric response in a glass-forming solvent: From picoseconds to seconds," *Chem. Phys. Lett.* **229**, 302–308 (1994).
- <sup>25</sup>A. I. Nielsen, T. Christensen, B. Jakobsen, K. Niss, N. B. Olsen, R. Richert, and J. C. Dyre, "Prevalence of approximate  $\tau$  relaxation for the dielectric  $\alpha$  process in viscous organic liquids," *J. Chem. Phys.* **130**, 154508 (2009).
- <sup>26</sup>S. F. Swallen, K. L. Kearns, M. K. Mapes, Y. S. Kim, R. J. McMahon, M. D. Ediger, T. Wu, L. Yu, and S. Satija, "Organic glasses with exceptional thermodynamic and kinetic stability," *Science* **315**, 353–356 (2007).
- <sup>27</sup>Y. Z. Chua, A. R. Young-Gonzales, R. Richert, M. D. Ediger, and C. Schick, "Dynamics of supercooled liquid and plastic crystalline ethanol: Dielectric relaxation and ac nanocalorimetry distinguish structural  $\alpha$ - and Debye relaxation processes," *J. Chem. Phys.* **147**, 014502 (2017).
- <sup>28</sup>T. Steiner, "Lengthening of the covalent X–H bond in heteronuclear hydrogen bonds quantified from organic and organometallic neutron crystal structures," *J. Phys. Chem. A* **102**, 7041–7052 (1998).
- <sup>29</sup>D. F. Aycock, "Solvent applications of 2-methyltetrahydrofuran in organometallic and biphasic reactions," *Org. Process Res. Dev.* **11**, 156–159 (2007).
- <sup>30</sup>R. L. David, *CRC Handbook of Chemistry and Physics*, 89th ed. (CRC Press, 2009).
- <sup>31</sup>See <https://www.sigmaaldrich.com/catalog/product/aldrich/478059?lang=en&region=US>, for Supplier information Sigma-Aldrich (2020).
- <sup>32</sup>S. Bauer, K. Burlafinger, C. Gainaru, P. Lunkenheimer, W. Hiller, A. Loidl, and R. Böhmer, "Debye relaxation and 250 K anomaly in glass forming monohydroxy alcohols," *J. Chem. Phys.* **138**, 094505 (2013).
- <sup>33</sup>S. Singh and J. J. de Pablo, "A molecular view of vapor deposited glasses," *J. Chem. Phys.* **134**, 194903 (2011).